



## VISIBILITY-MONOTONIC POLYGON DEFLATION

PROSENJIT BOSE, VIDA DUJMOVIĆ, NIMA HODA, AND PAT MORIN

**ABSTRACT.** A *deflated* polygon is a polygon with no visibility crossings. We answer a question posed by Devadoss et al. (2012) by presenting a polygon that cannot be deformed via continuous visibility-decreasing motion into a deflated polygon. We show that the least  $n$  for which there exists such an  $n$ -gon is seven. In order to demonstrate non-deflatability, we use a new combinatorial structure for polygons, the directed dual, which encodes the visibility properties of deflated polygons. We also show that any two deflated polygons with the same directed dual can be deformed, one into the other, through a visibility-preserving deformation.

## 1. INTRODUCTION

Much work has been done on visibilities of polygons [6, 9] as well as on their convexification, including work on convexification through continuous motions [4]. Devadoss et al. [5] combine these two areas in asking the following two questions: (1) Can every polygon be convexified through a deformation in which visibilities monotonically increase? (2) Can every polygon be deflated (i.e. lose all its visibility crossings) through a deformation in which visibilities monotonically decrease?

The first of these questions was answered in the affirmative at CCCG 2011 by Aichholzer et al. [2].

In this paper, we resolve the second question in the negative by presenting a non-deflatable polygon, shown in Figure 10A. While it is possible to use *ad hoc* arguments to demonstrate the non-deflatability of this polygon, we develop a combinatorial structure, the directed dual, that allows us to prove non-deflatability for this and other examples using only combinatorial arguments. We also show that seven is the least  $n$  for which there exists a non-deflatable  $n$ -gon in general position.

As a byproduct of developing the directed dual, we obtain the following additional results: (1) The vertex-edge visibility graph of a deflated polygon

---

Received by the editors September 27, 2012, and in revised form April 15, 2015.

2010 *Mathematics Subject Classification.* 52A10, 52C25.

*Key words and phrases.* Polygons, reconfiguration, deflation.

This research was partly funded by NSERC and the Ontario Ministry of Research and Innovation. The work of Nima Hoda was partly funded by Carleton University through an I-CUREUS research fellowship.

is completely determined by its directed dual; and (2) any deflated polygon may be monotonically deformed into any other deflated polygon having the same directed dual.

## 2. PRELIMINARIES

We begin by presenting some definitions. Here and throughout the paper, unless qualified otherwise, we take *polygon* to mean simple polygon on the plane.

A *triangulation*,  $T$ , of a polygon,  $P$ , with vertex set  $V$  is a partition of  $P$  into triangles with vertices in  $V$ . The *edges* of  $T$  are the edges of these triangles and we call such an edge a *polygon edge* if it belongs to the polygon or, else, a *diagonal*. A triangle of  $T$  with exactly one diagonal edge is an *ear* and the *helix* of an ear is its vertex not incident to any other triangle of  $T$ .

Let  $w$  and  $uv$  be a vertex and edge, respectively, of a polygon,  $P$ , such that  $u$  and  $v$  are seen in that order in a counter-clockwise walk along the boundary of  $P$ . Then  $uv$  is *facing*  $w$  if  $(u, v, w)$  is a left turn. Two vertices or a vertex and an edge of a polygon are *visible* or *see* each other if there exists a closed line segment contained inside the closed polygon joining them. If such a segment exists that intersects some other line segment then they are visible *through* the latter segment. We say that a polygon is in *general position* if the open line segment joining any of its visible pairs of vertices is contained in the open polygon.

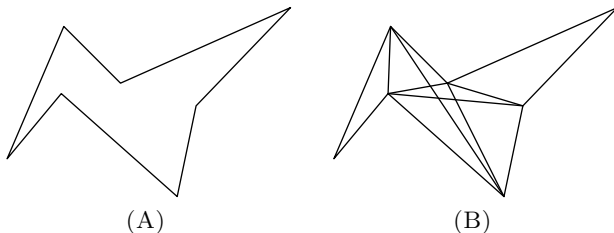


FIGURE 1. (A) A polygon and (B) its visibility graph.

The *visibility graph* of a polygon is the geometric graph on the plane with the same vertex set as the polygon and in which two vertices are connected by a straight open line segment if they are visible (e.g. see Figure 1).

**2.1. Polygon Deflation.** A *deformation* of a polygon,  $P$ , is a continuous, time-varying, simplicity-preserving transformation of  $P$ . Specifically, to each vertex,  $v$ , of  $P$ , a deformation assigns a continuous mapping  $t \mapsto v^t$  from the closed interval  $[0, 1] \subset \mathbb{R}$  to the plane such that  $v^0 = v$ . Additionally, for  $t \in [0, 1]$ ,  $P^t$  is simple, where  $P^t$  is the polygon joining the images of  $t$  in these mappings as their respective vertices are joined in  $P$ .

A *monotonic deformation* of  $P$  is one in which no two vertices ever become visible, i.e., there do not exist  $u$  and  $v$  in the vertex set of  $P$  and  $s, t \in [0, 1]$ ,

with  $s < t$ , such that  $u^t$  and  $v^t$  are visible in  $P^t$  but  $u^s$  and  $v^s$  are not visible in  $P^s$ .

A polygon is *deflated* if its visibility graph has no edge intersections. Note that a deflated polygon is in general position and that its visibility graph is its unique triangulation. Because of this uniqueness and for convenience, we, at times, refer to a deflated polygon and its triangulation interchangeably. A *deflation* of a polygon,  $P$ , is a monotonic deformation  $t \mapsto P^t$  of  $P$  such that  $P^1$  is deflated. If such a deformation exists, then  $P$  is *deflatable*.

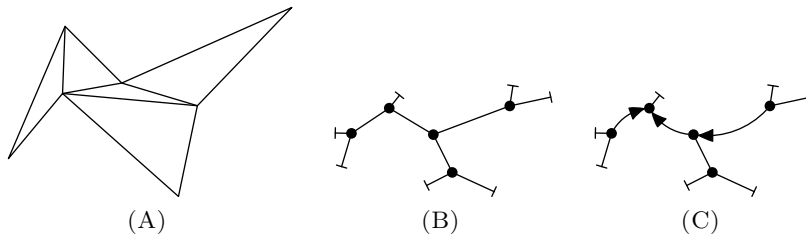


FIGURE 2. (A) A polygon triangulation, (B) its dual tree and (C) its directed dual. Triangle and terminal nodes are indicated with disks and tees, respectively.

**2.2. Dual Trees of Polygon Triangulations.** The *dual tree*,  $D$ , of a polygon triangulation,  $T$ , is a plane tree with a *triangle node* for each triangle of  $T$ , a *terminal node* for each polygon edge of  $T$  and where two nodes are adjacent if their correspondents in  $T$  share a common edge. The dual tree preserves edge orderings of  $T$  in the following sense. If a triangle,  $a$ , of  $T$  has edges  $e$ ,  $f$  and  $g$  in counter-clockwise order then the corresponding edges of its correspondent,  $a^D$ , in  $D$  are ordered  $e^D$ ,  $f^D$  and  $g^D$  in counter-clockwise order (e.g. see Figure 2B).

Note that the terminal and triangle nodes of a dual tree have degrees one and three, respectively. We call the edges of terminal nodes *terminal edges*.

An ordered pair of adjacent triangles  $(a, b)$  of a polygon triangulation,  $T$ , is *right-reflex* if the quadrilateral union of  $a$  and  $b$  has a reflex vertex,  $v$ , situated on the right-hand side of a single segment path from  $a$  to  $b$  contained in the open quadrilateral. We call  $v$  the *reflex endpoint* of the edge shared by  $a$  and  $b$  (see Figure 3).

The *directed dual*,  $D$ , of a polygon triangulation,  $T$ , is a dual tree of  $T$  that is partially directed such that, for every right-reflex pair of adjacent triangles  $(a, b)$  in  $T$ , the edge joining the triangle nodes of  $a$  and  $b$  in  $D$  is directed  $a \rightarrow b$  (e.g. see Figure 2C). Note that if  $P$  is deflated, then for every pair of adjacent triangles,  $(a, b)$ , of  $T$  one of  $(a, b)$  or  $(b, a)$  is right-reflex and so every non-terminal edge in  $D$  is directed.

Throughout this paper, as above, we use superscripts to denote corresponding objects in associated structures. For example, if  $a$  is a triangle of

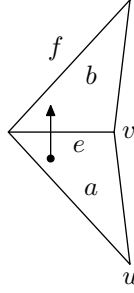


FIGURE 3. A pair of triangles,  $a$  and  $b$ , sharing an edge,  $e$ , such that their quadrilateral union has a reflex vertex and a single segment path from  $a$  to  $b$  contained in the open quadrilateral. The reflex endpoint,  $v$ , of  $e$  is to the right of the path and so the pair  $(a, b)$  is right-reflex.

the triangulation,  $T$ , of a polygon and  $b$  is a triangle node in the dual tree,  $D$ , of  $T$  then  $a^D$  and  $b^T$  denote the node corresponding to  $a$  in  $D$  and the triangle corresponding to  $b$  in  $T$ , respectively.

### 3. DIRECTED DUALS OF DEFLATED POLYGONS

In this section, we derive some properties of deflated polygons and use them to relate the visibilities of deflated polygons to paths in their directed duals. We also show that two deflated polygons with the same directed dual can be monotonically deformed into one another.

**Lemma 3.1.** *Let  $P$  be a deflated polygon, let  $a$  be an ear of  $P$  and let  $P'$  be the polygon resulting from removing  $a$  from  $P$ . Then  $P'$  is deflated.*

*Proof.*  $P'$  is a subset of  $P$ , so if a vertex pair is visible in  $P'$  then the corresponding pair is visible in  $P$ . Then a crossing in the visibility graph of  $P'$  would imply one in that of  $P$ .  $\square$

**Corollary 3.2.** *If the union of a subset of the triangles of a deflated polygon triangulation is a polygon, then it is deflated.*

**Lemma 3.3.** *If  $u$  is a vertex opposite a closed edge,  $e$ , in a triangle of a deflated polygon triangulation, then  $u$  sees exactly one polygon edge through  $e$ .*

*Proof.* If  $e$  is a polygon edge then  $u$  sees no other edge through  $e$  than  $e$  itself. Otherwise, if  $u$  saw more than one polygon edge through  $e$ , it would also see some vertex through  $e$ , implying a visibility crossing in the visibility graph of the deflated polygon—a contradiction.

Now, since the polygon is bounded, a sufficiently long open line segment starting on  $u$  and intersecting  $e$  must contain points both interior and exterior to the polygon. Then it must intersect the polygon boundary and, since

the polygon is deflated, the intersection point must be on an open polygon edge visible to  $u$ .  $\square$

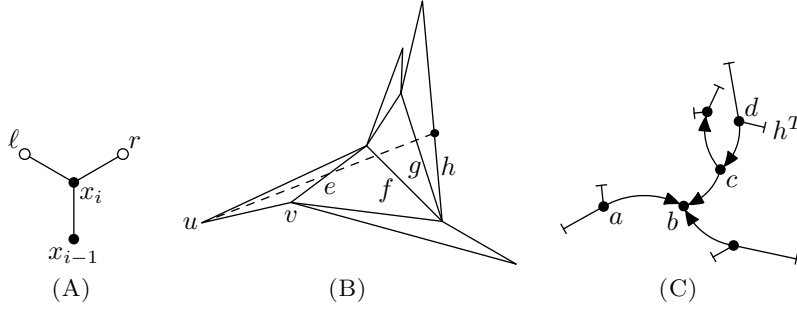


FIGURE 4. (A) A node  $x_i$  of a directed dual and its neighbours  $x_{i-1}$ ,  $r$  and  $\ell$  in an iteration of the construction of a visibility path, (B) a deflated polygon triangulation,  $T$ , wherein the induced sequence of the vertex  $u$  through the edge  $e$  is  $(e, f, g, h)$  and (C) the directed dual,  $T$ , in which the visibility path of the directed dual starting with nodes  $(a, b)$  is  $(a, b, c, d, h^T)$ .

Let  $u$  be the vertex of a deflated polygon triangulation,  $T$ , and let  $e$  be an edge opposite  $u$  in a triangle of  $T$ . An *induced sequence* of  $u$  through  $e$  is the sequence of edges through which  $u$  sees a polygon edge,  $f$ , through  $e$ . This sequence is ordered by the proximity to  $u$  of their intersections with a closed line segment joining  $u$  and  $f$  that is interior to the open polygon everywhere but at its endpoints (e.g. see Figure 4B).

**Lemma 3.4.** *Suppose  $u$  is a vertex opposite a closed non-polygon edge,  $e$ , in a triangle,  $a$ , of a deflated polygon triangulation. Let  $v$  be the reflex endpoint of  $e$  and let  $f$  be the edge opposite  $v$  in the triangle sharing  $e$  with  $a$  (see Figure 3). Then  $u$  sees the same polygon edge through  $e$  as  $v$  sees through  $f$ .*

*Proof.* The ray from  $u$  through  $v$  intersects  $f$ . Then, if  $f$  is a polygon edge,  $u$  sees it. Otherwise,  $f$  is a diagonal and the ray intersects some other polygon edge visible to both  $u$  and  $v$ . From Lemma 3.3, we have the uniqueness of the edge  $u$  sees through  $f$ , which completes the proof.  $\square$

**Corollary 3.5.** *If  $u$ ,  $v$ ,  $e$  and  $f$  are as in Lemma 3.4, then the induced sequence of  $u$  through  $e$  is equal to that of  $v$  through  $f$  prepended with  $e$ .*

*Proof.* This follows from Lemma 3.4 and Corollary 3.2.  $\square$

**3.1. Directed Duals and Visibility.** A *visibility path*,  $(x_1, x_2, \dots, x_n)$ , of the *directed dual*,  $D$ , of a deflated polygon is a sequence of nodes in  $D$  meeting the following conditions.  $x_1$  is a triangle node adjacent to  $x_2$  and,

for  $i \in \{2, \dots, n\}$ , if  $x_i$  is a terminal node, then it is  $x_n$ —the final node of the path. Otherwise, let the neighbours of  $x_i$  be  $x_{i-1}$ ,  $r$  and  $\ell$  in counter-clockwise order (see Figure 4A). Then

$$x_{i+1} = \begin{cases} r & \text{if edge } \{x_{i-1}, x_i\} \text{ is directed } x_{i-1} \leftarrow x_i \\ \ell & \text{if edge } \{x_{i-1}, x_i\} \text{ is directed } x_{i-1} \rightarrow x_i \end{cases}$$

(e.g. see Figure 4C).

Note that two consecutive nodes of a visibility path determine all subsequent nodes and so any suffix of length greater than one of a visibility path is also a visibility path.

**Lemma 3.6.** *Let  $(a, b, c)$  be a simple path in the directed dual,  $D$ , of a deflated polygon triangulation,  $T$ , where  $a$  and  $b$  are triangle nodes joined by the edge  $e$ . Let  $u$  be the vertex opposite  $e^T$  in  $a^T$ , let  $v$  be the reflex endpoint of  $e^T$  and let  $f$  be the edge opposite  $v$  in  $b^T$  (see Figure 4B). Then  $(a, b, c)$  is the substring of a visibility path if and only if  $f^D$  joins  $b$  and  $c$  in  $D$ .*

*Proof.* Suppose  $(a, b, c)$  is the substring of a visibility path and let  $x$  be the neighbour of  $b$  not  $a$  nor  $c$  and let  $x'$  be the edge of  $b^T$  not  $e^T$  nor  $f$ . We consider the case where the neighbours of  $b$  are  $a$ ,  $x$  and  $c$  in counter-clockwise order—the argument is symmetric in the other case. Then  $(a, b)$  is right-reflex and so  $b^T$  has counter-clockwise edge ordering:  $e^T$ ,  $x'$ ,  $f$ . Then, since edge orderings are preserved in the directed dual,  $f^D$  joins  $b$  and  $c$  as required. Reversing the argument gives the converse.  $\square$

**Corollary 3.7.** *Let  $D$ ,  $T$ ,  $a$ ,  $b$ ,  $e$  and  $u$  be as in Lemma 3.6. The induced sequence of  $u$  through  $e$  is equal to the sequence of correspondents in  $T$  of edges traversed by the visibility path starting with  $(a, b)$  in  $D$ . The final node of this visibility path corresponds to the edge  $u$  sees through  $e^T$ .*

*Proof.* This follows, by induction, from Lemma 3.6 and Corollary 3.5.  $\square$

**Theorem 3.8.** *A vertex,  $u$ , and edge,  $g$ , of a deflated polygon,  $P$ , are visible if and only if there is a visibility path in the directed dual,  $D$ , of the triangulation,  $T$ , of  $P$  starting on a triangle node corresponding to a triangle incident to  $u$  and ending on  $g^D$ .*

*Proof.* Assume  $u$  sees  $g$ . If  $g$  is an edge of a triangle,  $a$ , incident to  $u$  then  $(a^D, g^D)$  is the required visibility path. Otherwise  $u$  sees  $g$  through some edge,  $e$ , and the existence of the required visibility path follows from Corollary 3.7.

Assume, now, that the visibility path exists. If its triangle nodes all correspond to triangles incident to  $u$  then  $g$  is incident to one of these triangles and so visible to  $u$ . Otherwise, let  $e$  be the first edge the path traverses from a node,  $a$ , corresponding to a triangle incident to  $u$  to a node,  $b$ , corresponding to a triangle not incident to  $u$ .

Then, by Corollary 3.7, the induced sequence of  $u$  through  $e^T$  corresponds to a visibility path starting with  $(a, b)$  and this visibility path ends on a node

corresponding to the edge  $u$  sees through  $e$ . Since two consecutive nodes of a visibility path determine all subsequent nodes, these visibility paths end on the same node,  $g^D$ , and so  $u$  sees  $g$ .  $\square$

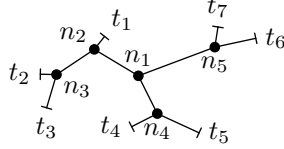


FIGURE 5. A plane tree with the following maximal outer paths:  $(t_7, n_5, n_1, n_2, t_1)$ ,  $(t_1, n_2, n_3, t_2)$ ,  $(t_2, n_3, t_3)$ ,  $(t_3, n_3, n_2, n_1, n_4, t_4)$ ,  $(t_4, n_4, t_5)$ ,  $(t_5, n_4, n_1, n_5, t_6)$ ,  $(t_6, n_5, t_7)$ .

An *outer path* of a plane tree,  $D$ , is the sequence of nodes visited in a counter-clockwise walk along its outer face in which no node is visited twice. An outer path is *maximal* if it is not a proper substring of any other outer path (e.g. see Figure 5). Note that an outer path,  $(x_1, x_2, \dots, x_n)$ , of the directed dual of a polygon triangulation,  $T$ , corresponds to a triangle fan in  $T$  where the triangles have clockwise order  $x_1^T, x_2^T, \dots, x_n^T$  about their shared vertex.

**Theorem 3.9.** *A pair of vertices,  $u$  and  $v$ , of a deflated polygon  $P$  are visible if and only if, in the directed dual,  $D$ , of the triangulation,  $T$ , of  $P$ , their corresponding maximal outer paths share a node.*

*Proof.* The maximal outer paths of  $u$  and  $v$  share a node in  $D$  if and only if they are incident to a common triangle in  $T$  and, since  $P$  is deflated, this is the case if and only if  $u$  and  $v$  are visible.  $\square$

**3.2. Directed Dual Equivalence.** In this section, we show that if two deflated polygons have the same directed dual, then one can be monotonically deformed into the other. First, we fully characterize the directed duals of deflated polygons.

**Theorem 3.10.** *A partially directed plane tree,  $D$ , in which every non-terminal node has degree three and where an edge is directed if and only if it joins two non-terminal nodes of degree three is the directed dual of a deflated polygon if and only if it does not contain an outer path,  $(x_1, x_2, \dots, x_n)$ , with  $n \geq 4$ , such that the edges from  $x_1$  and  $x_{n-1}$  are both forward directed (i.e.  $x_1 \rightarrow x_2$  and  $x_{n-1} \rightarrow x_n$ ).*

Henceforth, we call such a path an *illegal path*.

*Proof.* Suppose  $D$  contains an illegal path,  $(x_1, x_2, \dots, x_n)$ . If  $D$  is the directed dual of a polygon triangulation,  $T$ , then  $x_1^T, x_2^T, x_{n-1}^T$  and  $x_n^T$  share a common reflex vertex in both quadrilaterals  $x_1^T \cup x_2^T$  and  $x_{n-1}^T \cup x_n^T$  (see Figure 6). This contradicts the disjointness of these quadrilaterals.

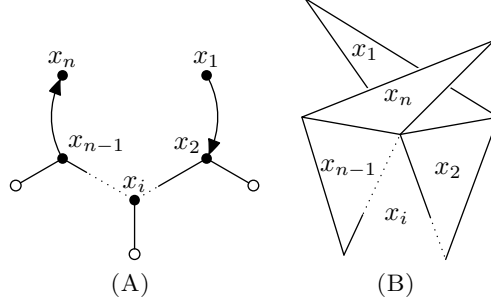


FIGURE 6. If (A) the tree with outer path  $(x_1, x_2, \dots, x_n)$  were a subtree of the directed dual of a polygon triangulation,  $T$ , then (B) the triangles corresponding to nodes  $x_1, x_2, x_{n-1}$  and  $x_n$  in  $T$  would overlap, contradicting the simplicity of the polygon.

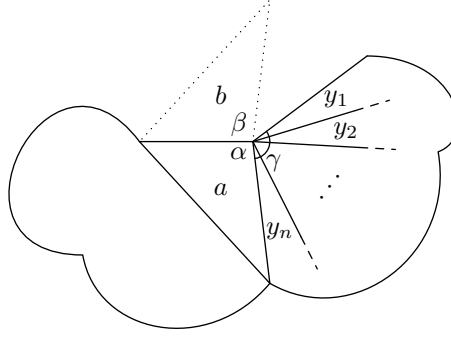


FIGURE 7. The inductive polygon in the proof of Theorem 3.10 or a polygon from the inductive deformation in the proof of Theorem 3.11.

Suppose, now, that  $D$  has no illegal paths. We prove the converse with a construction of a polygon triangulation having  $D$  as its directed dual. Let  $b$  be a terminal node in the subtree of  $D$  induced by its non-terminal nodes. Then  $b$  has two terminal neighbours and one non-terminal neighbour,  $a$ . Let  $D'$  be the tree resulting from replacing  $a$  and its terminal neighbours with a single terminal node,  $x$ , connected to  $b$  with an undirected edge. By induction on the number of non-terminal nodes, there exists a deflated polygon triangulation,  $T$ , having  $D'$  as its directed dual.

Assume, without loss of generality, that the edge joining  $a$  and  $b$  is directed  $a \rightarrow b$ . Let  $u$  be the endpoint of  $x^T$  pointing in a clockwise direction in the boundary of  $T$  and let  $(y_1, y_2, \dots, y_n)$  be the outer path of  $D$  corresponding to the triangles other than  $b^T$  in  $T$  incident to  $u$  (see Figure 7). Note that  $(y_i, y_{i+1}, \dots, y_n, a, b)$  is an outer path of  $D$  and so, by hypothesis, for all  $i \in \{1, 2, \dots, n-1\}$ , the edge joining  $y_i$  and  $y_{i+1}$  is directed  $y_i \leftarrow y_{i+1}$ .



Then, to show that a triangle may be appended to  $T$  to form the required triangulation, it suffices to show that the sum of the angles at  $u$  of the triangles  $y_1^T, y_2^T, \dots, y_n^T$  is less than  $\pi$ , which, in turn, follows from the backward directedness of the edges of  $(y_1, y_2, \dots, y_n)$ .  $\square$

**Theorem 3.11.** *If the deflated polygons  $P$  and  $P'$  have the same directed dual,  $D$ , then  $P$  can be monotonically deformed into  $P'$ .*

*Proof.* Let  $b$  be an ear of the triangulation,  $T$ , of  $P$  and let  $b'$  be the triangle corresponding to  $b^D$  in the triangulation,  $T'$ , of  $P'$ . By induction on the number of triangles in  $T$ , there is a monotonic deformation  $t \mapsto Q^t$  from  $Q = P \setminus b$  to  $Q' = P' \setminus b'$ . Note that replacing  $b^D$  and its terminal nodes in  $D$  with a single terminal node gives the directed dual,  $D'$ , of  $Q$ . Then, since  $Q$  is deflated (Lemma 3.1) and  $t \mapsto Q^t$  is monotonic, for all  $t \in [0, 1]$ ,  $Q^t$  is deflated and has directed dual  $D'$ .

Let  $v$  be the helix of  $b$ , let  $a$  be the triangle sharing an edge,  $e$ , with  $b$  and let  $u$  be the reflex endpoint of  $e$ . We need to show that there is a continuous map  $t \mapsto v^t$  that, combined with  $t \mapsto Q$ , gives a monotonic deformation of a polygon with directed dual  $D$ . For  $t \in [0, 1]$ , let  $\alpha^t$  be the angle of  $a^t$  at  $u^t$  in  $Q^t$  and let  $\gamma^t$  be the sum of the angles at  $u^t$  of the triangles,  $y_1^t, y_2^t, \dots, y_n^t$ , other than  $a^t$  of the triangulation of  $Q^t$  incident to  $u^t$  (see Figure 7).

Then, since  $v$  may be brought arbitrarily close to  $u$  in a monotonic deformation of  $P$ , it suffices to show that there is a continuous map  $t \mapsto \beta^t$  specifying an angle for  $b^t$  at  $u^t$  such that, for all  $t \in [0, 1]$ ,  $0 < \beta^t < \pi$ ,  $\alpha^t + \beta^t > \pi$  and  $\alpha^t + \beta^t + \gamma^t < 2\pi$ . The latter two conditions are equivalent to

$$\pi - \alpha^t < \beta^t < (\pi - \alpha^t) + (\pi - \gamma^t).$$

It follows from Theorem 3.10 that the outer path  $(y_1^{D'}, y_2^{D'}, \dots, y_n^{D'})$  is left-directed and so that  $\gamma^t < \pi$ . Then  $\beta^t = \pi - (\alpha^t + \gamma^t)/2$  satisfies all required conditions.

Now, let  $t \mapsto R^t$  be the monotonic deformation from a polygon with directed dual  $D$  combining  $t \mapsto Q^t$  and the map  $t \mapsto v^t$  defined by a fixed distance between  $u^t$  and  $v^t$  of  $r \in \mathbb{R}_{>0}$  and an angle for  $b^t$  at  $u^t$  of  $\beta^t$ .

Prepending  $t \mapsto R^t$  with a deformation of  $P$  in which  $v$  is brought to the distance  $r$  from  $u$  and then rotated about  $u$  to an angle of  $\beta^0$ ; then appending a deformation comprising similar motions ending at  $P'$ ; and, finally, scaling in time gives a continuous map,  $t \mapsto P^t$ , with  $P^0 = P$  and  $P^1 = P'$ . Since, for all  $t \in [0, 1]$ ,  $Q^t$  is simple, a small enough  $r$  can be chosen such that  $t \mapsto P^t$  is simplicity-preserving. Then, by the properties of  $t \mapsto \beta^t$ ,  $t \mapsto P^t$  is the required monotonic deformation.  $\square$

#### 4. VERTEX-EDGE VISIBILITIES IN MONOTONIC DEFORMATIONS

In the following Lemmas we use analytic arguments similar to those used by Ábrego et al. [1] to investigate the nature of collinearities in deformations and derive a needed vertex-edge visibility property of monotonic deformations.

**Lemma 4.1.** *Let  $t \mapsto P^t$  be a deformation of a polygon,  $P$ , let  $u, v$  and  $w$  be vertices of  $P$  and let  $c \in [0, 1]$ . Suppose that, for every  $\delta > 0$ , the pierced  $\delta$ -neighbourhood,  $N_\delta = (c - \delta, c + \delta) \cap [0, 1] \setminus \{c\}$ , of  $c$  has a point,  $s \in N_\delta$ , such that  $u^s, v^s$  and  $w^s$  are collinear in  $P^s$ . Then  $u^c, v^c$  and  $w^c$  are collinear in  $P^c$ .*

*Proof.* Assume otherwise and, for all  $t \in [0, 1]$ , let  $\alpha^t$  be the angle between  $u^t, v^t$  and  $w^t$  in  $P^t$ . Then  $t \mapsto \alpha^t$  is continuous and  $\alpha^c \neq k\pi$ , for any  $k \in \mathbb{Z}$ . Then, by hypothesis, there is no  $\delta > 0$  such that, for all  $t \in N_\delta$ ,  $|\alpha^c - \alpha^t| < \min_{k \in \mathbb{Z}} |\alpha^c - k\pi| > 0$ , contradicting the continuity of  $t \mapsto \alpha^t$ .  $\square$

**Corollary 4.2.** *Let  $t \mapsto P^t$  be a deformation of a polygon,  $P$ , let  $u, v$  and  $w$  be vertices of  $P$  and let  $c \in [0, 1]$ . If  $u^c, v^c$  and  $w^c$  are not collinear in  $P^c$ , then there exists a  $\delta > 0$  such that, for every  $t \in N_\delta$ ,  $u^t, v^t$  and  $w^t$  are not collinear in  $P^t$ .*

**Corollary 4.3.** *Let  $t \mapsto P^t$  be a deformation of a polygon,  $P$ , and let  $c \in [0, 1]$ . There exists a  $\delta > 0$  such that, for every  $t \in N_\delta$ , no three vertices are collinear in  $P^t$  unless their correspondents are collinear in  $P^c$ .*

We call the corresponding  $\delta$ -neighbourhood,  $N_\delta$ , the *safe neighbourhood* of  $c$ .

**Lemma 4.4.** *Let  $t \mapsto P^t$  be a deformation of a polygon,  $P$ , let  $u$  be a vertex of  $P$ , let  $c \in [0, 1]$ , let  $N_\delta$  be a safe neighbourhood of  $c$  and let  $W^c$  be a subset of the vertices of  $P^c$  having distinct projections onto the unit circle about  $u^c$ . Then, for all  $t \in N_\delta$ , the corresponding vertex subset,  $W^t$ , of  $P^t$  has the same radial order about  $u^t$  as does  $W^c$  about  $u^c$ .*

*Proof.* Since deformations preserve simplicity, the vertices of  $P^t$  never coincide and so their projections on the unit circle about  $u^t$  also move continuously. Then a change in radial order between two vertices, say  $v$  and  $w$ , implies that, for some intermediate  $c' \in (c, t)$ ,  $u^{c'}, v^{c'}$  are  $w^{c'}$  collinear in  $P^{c'}$ , contradicting  $N_\delta$  being a safe neighbourhood.  $\square$

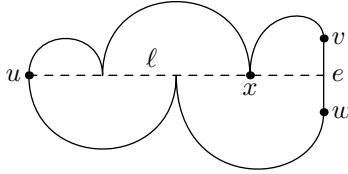


FIGURE 8. A polygon with visible vertex-edge pair,  $(u, e)$ , joined by a unique closed line segment,  $\ell$ , contained in the closed polygon.

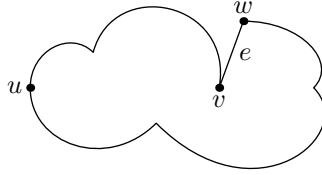


FIGURE 9. A polygon in general position in which a vertex,  $u$ , and edge,  $e$ , are not visible and where  $u$  sees a single endpoint,  $v$ , of  $e$ . In such a polygon,  $e$  necessarily neither faces nor is collinear to  $u$ .

## 5. DEFLATABILITY OF POLYGONS

In this section, we show how deflatable polygons may be related combinatorially to their deflation targets and use this result to present a polygon that cannot be deflated. We also show that vertex-vertex visibilities do not determine deflatability. These results depend on the following Lemma.

**Lemma 5.1.** *Let  $t \mapsto P^t$  be a monotonic deformation of a polygon,  $P$ , in general position. Then a vertex and an edge are visible in  $P^1$  only if they are visible in  $P$ .*

*Proof.* Suppose a vertex,  $u^1$ , sees an edge,  $e^1$ , with endpoints  $v^1$  and  $w^1$  in  $P^1$  such that  $u$  and  $e$  are not visible in  $P$ . Let  $c$  be the supremum of the set

$$\{x \in [0, 1] : \text{for all } t \in [0, x), u^t \text{ and } e^t \text{ are not visible in } P^t\}$$

and let  $N_\delta$  be a safe neighbourhood of  $c$  (Corollary 4.3). Note that  $e^c$  is either facing  $u^c$  or is collinear with  $u^c$  in  $P^c$ , since, otherwise, for all  $t \in N_\delta$ ,  $u^t$  and  $e^t$  would not be visible in  $P^t$ , contradicting the choice of  $c$ .

We begin by establishing the claim that there exists a unique closed line segment,  $\ell$ , contained in the closed polygon  $P^c$  joining  $u^c$  and the closed edge  $e^c$ . Suppose, first, that no such segment exists. Then every open line segment joining  $u^c$  and  $e^c$  intersects an open edge of  $P^c$ . Then, by Lemma 4.4, for all  $t \in N_\delta$ ,  $u^t$  and  $e^t$  are not visible in  $P^t$ , contradicting the choice of  $c$ .

Suppose, now, that two such segments exist. Then either these segments are collinear, in which case so are  $u^c$  and the endpoints of  $e^c$ , contradicting the monotonicity of the deformation (since  $u$  may see at most a single endpoint of  $e$  in  $P$  without seeing  $e$  itself) or else they form a triangle. Then every closed segment joining  $u^c$  and  $e^c$  contained in this closed triangle is also such a segment and so, by Lemma 4.4, for all  $t \in N_\delta$ ,  $u^t$  and  $e^t$  are visible in  $P^t$ , contradicting the choice of  $c$ .

From the claim, it follows that  $e^c$  is facing  $u^c$  in  $P^c$  and we are left with two cases.

**Case I:**  $\ell$  joins  $u^c$  and a point on the open edge  $e^c$ . Since  $\ell$  is unique, there is at least one vertex from each of the two chains of  $P^c$  from  $u^c$  to  $e^c$  incident

to  $\ell$ , as in Figure 8. Let  $x^c$  be the furthest of these vertices from  $u^c$  and let  $s \in N_\delta$ , with  $s < c$ . Suppose  $u^s$  and  $x^s$  are visible in  $P^s$ . Then the closed line segment joining  $u^s$  and  $x^s$  is contained in the closed polygon  $P^s$  but, since  $s < c$ , the extension of this segment joining  $x^s$  and  $e^s$  must intersect an open edge  $f^s$  of  $P^s$ . It, then, follows from Lemma 4.4 that an endpoint of  $f^c$  is incident to  $\ell$  in  $P^c$  between  $x^c$  and  $e^c$ , contradicting the choice of  $x^c$ . Then  $u^s$  and  $x^s$  are not visible in  $P^s$  but  $u^c$  and  $x^c$  are visible in  $P^c$ , contradicting the monotonicity of the deformation.

**Case II:**  $\ell$  joins  $u^c$  and an endpoint, say  $v^c$  without loss of generality, of  $e^c$ . Then  $u^c$  sees  $v^c$  in  $P^c$  and so, by monotonicity, for all  $t \in [0, c)$ ,  $u^t$  sees  $v^t$  in  $P^t$ . Since  $P$  is in general position and  $u$  and  $e$  are not visible in  $P$ ,  $e$  must neither be facing  $u$  nor be collinear with  $u$  in  $P$ , as in Figure 9. Then, since  $e^c$  is facing  $u^c$  in  $P^c$ , there must be some intermediate  $c' \in (0, c)$  such that  $u^{c'}$  and  $e^{c'}$  are collinear in  $P^{c'}$ . But since  $u^{c'}$  sees  $v^{c'}$  in  $P^{c'}$ , it must also see the other endpoint,  $w^{c'}$ , of  $e^{c'}$ , contradicting the monotonicity of the deformation.  $\square$

## 6. DEFLATABILITY OF POLYGONS

With this result, we now show how deflatable polygons may be related combinatorially to their deflation targets and use this result to present a polygon that cannot be deflated. We also show that vertex-vertex visibilities do not determine deflatability.

A *compatible directed dual* of a polygon,  $P$ , in general position is the directed dual of a deflated polygon,  $P'$ , such that, under an order- and chirality-preserving bijection between the vertices of  $P$  and  $P'$ , a vertex-edge or vertex-vertex pair are visible in  $P'$  only if their correspondents are visible in  $P$ . By *chirality*-preserving bijection, we mean one under which a counter-clockwise walk on the boundary of  $P$  corresponds to a counter-clockwise walk on the boundary of  $P'$ .

**Theorem 6.1.** *A polygon,  $P$ , in general position with no compatible directed dual is not deflatable.*

*Proof.* It follows from Lemma 5.1 that if  $P$  is monotonically deformable to a deflated polygon  $P'$ , then the directed dual of  $P'$  is compatible with  $P$ .  $\square$

**Lemma 6.2.** *Suppose a polygon,  $P$ , in general position has a compatible directed dual,  $D$ . Let  $P'$  be the deflated polygon with directed dual  $D$  whose vertex-vertex and vertex-edge visibilities are a subset of those of  $P$  under an order- and chirality-preserving bijection. Then the unique triangulation,  $T'$ , of  $P'$  is a triangulation,  $T$ , of  $P$  under the bijection and  $D$  can be constructed by directing the undirected non-terminal edges of the directed dual of  $T$ .*

*Proof.* Note that  $T'$  is the visibility graph of  $P'$ . Then, since  $P$  is in general position and has the same vertex count as  $P'$ , it follows from the vertex-vertex visibility subset property of  $P'$  that  $T'$  triangulates  $P$  under the bijection.

It remains to show that, for every non-terminal edge of the directed dual of  $T$ , either the edge is undirected or it is directed as in  $D$  or, equivalently, that for every pair of adjacent triangles,  $a$  and  $b$ , in  $T$  corresponding to the triangles  $a'$  and  $b'$  in  $T'$ , if  $(a, b)$  is right-reflex then so is  $(a', b')$ . Suppose, instead, that  $(b', a')$  is right-reflex. Let  $e'$  be the edge shared by  $a'$  and  $b'$ , let  $u'$  be the vertex of  $a'$  opposite  $e'$  and let  $f'$  be the edge of  $b'$  opposite the reflex endpoint of  $e'$ . Then, by Lemma 3.4,  $u'$  sees an edge through  $f'$  but the corresponding visibility is not present in  $P$ , contradicting the vertex-edge visibility subset property of  $P'$ .  $\square$

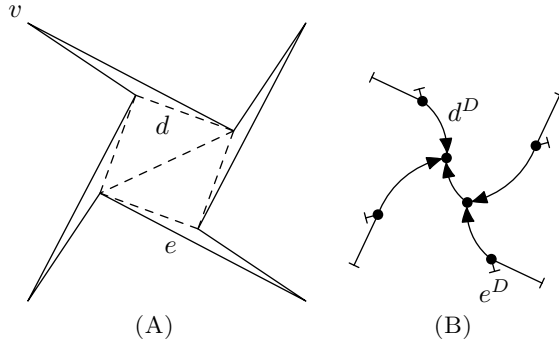


FIGURE 10. (A) A non-deflatable polygon,  $P$ , with its only triangulation, up to symmetry, indicated with dashed lines and (B) its only candidate for a compatible directed dual,  $D$ , up to symmetry.

**Theorem 6.3.** *There exists a polygon that cannot be deflated.*

*Proof.* We show that the general position polygon,  $P$ , in Figure 10A has no compatible directed dual and so, by Theorem 6.1, is not deflatable. Assume that the directed dual,  $D$ , of a deflated polygon,  $P'$ , is compatible with  $P$ . Then, by Lemma 6.2,  $D$  can be constructed by directing the undirected non-terminal edges of the directed dual of some triangulation of  $P$ . Up to symmetry,  $P$  has a single triangulation, its directed dual has a single undirected non-terminal edge and there is a single way to direct this edge. Then we may assume, without loss of generality, that  $D$  is the tree shown in Figure 10B and, by Theorem 3.8, the correspondents of the vertex  $v$  and edge  $e$  in  $P'$  are visible. This contradicts the compatibility of  $D$ .  $\square$

This combinatorial technique of using the non-existence of compatible directed duals can also be applied to other polygons. For example, the heptagon whose unique triangulation (up to symmetry) is shown in Figure 11A can also be shown to be non-deflatable in this way, as can the nonagon of Figure 12.

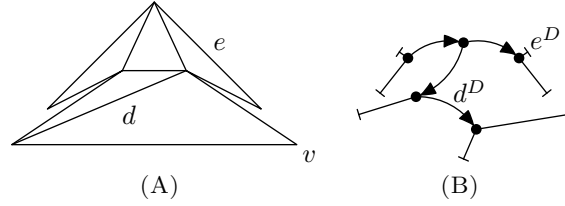


FIGURE 11. (A) The only triangulation, up to symmetry, of a non-deflatable heptagon and (B) its only candidate for a compatible directed dual,  $D$ .

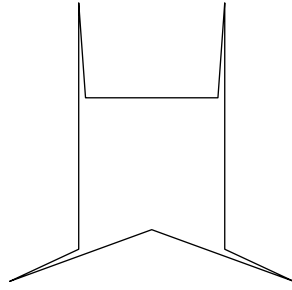


FIGURE 12. A non-deflatable nonagon.

Specifically, the directed dual of the triangulation of the heptagon,  $P$ , leaves only a single non-terminal edge undirected. By Theorem 3.10, this edge may be directed in only one way such that the resulting directed dual,  $D$ , shown in Figure 11B, has no illegal paths and is thus the directed dual of a deflated polygon,  $P'$ . Then the correspondents of  $v$  and  $e$  are visible in  $P'$  so that  $D$  is incompatible with  $P$ . The non-deflatability proof for the nonagon must consider two triangulations but has the same general form.

A natural question is: What is the least  $n$  for which there exists a non-deflatable  $n$ -gon in general position? It is trivial to show that every quadrilateral is deflatable and not difficult to show the same for all general position pentagons. Then it remains only to check for the existence of a non-deflatable hexagon.

**Theorem 6.4.** *Every general position hexagon is monotonically deflatable.*

*Proof.* Let  $P$  be any hexagon in general position. The proof is by induction on the number,  $m$ , of pairs of mutually visible non-adjacent vertices of  $P$ . The base case,  $m = 3$ , happens when the hexagon is already deflated (it has a unique triangulation with four triangles and three non-polygon edges).

The inductive step is made using an enormous case analysis grouped by the number of reflex vertices of the hexagon. Note that the vertex set of a general position hexagon (segments joining visible vertex pairs are interior to the hexagon) may be put into point set general position (no three points

are collinear) through a visibility-preserving perturbation. Thus we may assume in this step that the vertex set of  $P$  is in general position.

The case where  $P$  has no reflex vertices is handled by moving a vertex inwards until it becomes reflex. A simple argument, presented in the next paragraph, suffices to handle all cases in which  $P$  has exactly one reflex vertex.

Refer to Figure 13 for what follows. Let  $a, b, c, d, e$ , and  $f$  be the vertices of  $P$  in the order they occur on the boundary of  $P$  and suppose, without loss of generality, that  $a$  is the unique reflex vertex of  $P$ . Suppose, again without loss of generality that there is a closed halfplane with  $a$  on its boundary that contains  $a, b, c$ , and  $d$ , but not  $f$ . Then  $abcd$  is a convex quadrilateral contained in  $P$  and moving  $c$  directly towards  $a$  until it crosses  $bd$  removes at least one visible pair, namely  $bd$ , from  $P$ . This motion is monotonic because the only vertices not visible from  $c$  (possibly  $f$  and  $e$ ) remain hidden “behind”  $a$ . In particular, the orientations of the triangles  $fac$  and  $eac$  do not change during this motion.

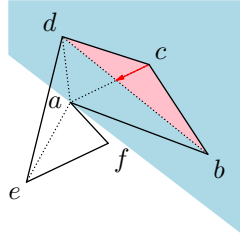


FIGURE 13. The inductive step of Theorem 6.4 when  $P$  has one reflex vertex.

The remaining cases have 2 or 3 reflex vertices and are each handled using a motion illustrated in Appendix A. All these motions move a single vertex, say  $a$ , along a linear trajectory until it crosses a segment joining a visible pair of vertices in  $P$ . All these motions have two properties that make it easy to check their correctness:

- (1) There is a convex polygon,  $C$ , whose vertices are a subset of those of  $P$ , that contains  $a, b$ , and  $f$ . Additionally, the closure of  $C$  contains  $ab$  and  $af$ , while its interior intersects the boundary of  $P$  at most in  $ab$  and  $af$ . Throughout the motion,  $a$  remains within  $C$ , except at the end, where it passes through the interior of an edge of  $C$  that is interior to  $P$  and stops an arbitrarily small distance outside of  $C$ . This guarantees that  $P$  remains simple throughout the motion. (See Figure 14, where  $C$  is the triangle  $bcf$ .)
- (2) The motion of  $a$  is such that the region bounded by the polygon strictly loses points, i.e.,  $P^{t'} \subsetneq P^t$  for all  $0 \leq t \leq t' \leq 1$ . This ensures that no pair of vertices  $x, y \in \{b, c, d, e, f\}$  ever becomes visible during the motion. That is, the only possibility of the motion

being non-monotonic comes from the possibility that  $a$  may gain visibilities as it moves.

The only remaining check, for each case, is to ensure that no new visible pair involving  $a$  appears during the motion. This can be done case by case using only order type information about  $P$ . We now illustrate one example, in Figure 14. In this example,  $a$  is moved toward the interior of  $P$  along the line through  $ab$  until it crosses the segment  $fc$ . This eliminates the visible pair  $fc$ . This motion satisfies properties 1 and 2, above, so the polygon remains simple throughout the motion and no new visible pairs not involving  $a$  are created. To check that no new visible pair involving  $a$  is created during the motion, observe that, initially, the only vertex not visible from  $a$  is  $e$ . In particular, this is because the sequence  $efa$  forms a right turn. This remains true at the end of the motion because  $efc$  forms a right turn and, at the end of the motion,  $a$  is arbitrarily close to the segment  $fc$ . Therefore, by convexity,  $efa$  forms a right turn throughout the motion and at no point during the motion does the pair  $ae$  become visible.

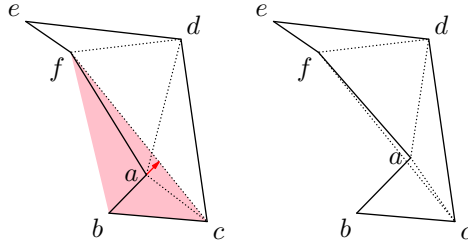


FIGURE 14. One of the cases where  $P$  has more than one reflex vertex in the proof of Theorem 6.4.

Similar statements can be verified for all the polygons in Appendix A. We wish the reader good luck with their verification.  $\square$

**Theorem 6.5.** *The vertex-vertex visibilities of a polygon do not determine its deflatability.*

*Proof.* The polygon in Figure 15 has the same vertex-vertex visibilities as the non-deflatable polygon in Figure 10A and yet can be deflated by moving the vertex  $u$  through the diagonal  $f$ .  $\square$

## 7. SUMMARY AND CONCLUSION

We presented the directed dual and showed that it captures the visibility properties of deflated polygons. We then showed that two deflated polygons with the same directed dual can be monotonically deformed into one another. Next, we showed that directed duals can be used to reason combinatorially, via directed dual compatibility, about the deflatability of polygons. Finally, we presented a polygon that cannot be deflated, showed that a non-deflatable



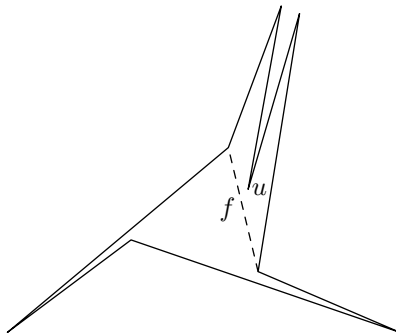


FIGURE 15. A deflatable polygon with the same vertex-vertex visibilities as the non-deflatable polygon shown in Figure 10A.

general position polygon must have at least seven vertices and showed that the vertex-vertex visibilities of a polygon do not determine its deflatability.

A full characterization of deflatable polygons still remains to be found. If the converse of Theorem 6.1 is true, then the existence of a compatible directed dual gives such a characterization. We conjecture the following weaker statement.

**Conjecture.** *The vertex-edge visibilities of a polygon in general position determine its deflatability.*

We conclude, however, by noting that, in light of Mnev’s Universality Theorem [8], it is unknown if even the order type of a polygon’s vertex set determines its deflatability.

## REFERENCES

1. B. M. Ábrego, M. Cetina, J. Leños, and G. Salazar, *Visibility-preserving convexifications using single-vertex moves*, Inform. Process. Lett. **112** (2012), no. 5, 161–163.
2. O. Aichholzer, G. Aloupis, E. D. Demaine, M. L. Demaine, V. Dujmović, F. Hurtado, A. Lubiw, G. Rote, A. Schulz, D. L. Souvaine, and A. Winslow, *Convexifying polygons without losing visibilities*, Proc. 23rd Annual Canadian Conference on Computational Geometry (CCCG), 2011, pp. 229–234.
3. O. Aichholzer, F. Aurenhammer, and H. Krasser, *Enumerating order types for small point sets with applications*, Order **19** (2002), no. 3, 265–281.
4. R. Connelly, E. D. Demaine, and G. Rote, *Straightening polygonal arcs and convexifying polygonal cycles*, Proceedings of the 41st Annual Symposium on Foundations of Computer Science, 2000, pp. 229–234.
5. S. L. Devadoss, R. I. Shah, X. Shao, and E. Winston, *Deformations of associahedra and visibility graphs*, Contrib. Discrete Math. **7** (2012), no. 1, 68–81.
6. S. K. Ghosh, *Visibility algorithms in the plane*, Cambridge University Press, Cambridge, 2007.
7. J. E. Goodman and R. Pollack, *Multidimensional sorting*, SIAM J. Comput. **12** (1983), no. 3, 484–507.

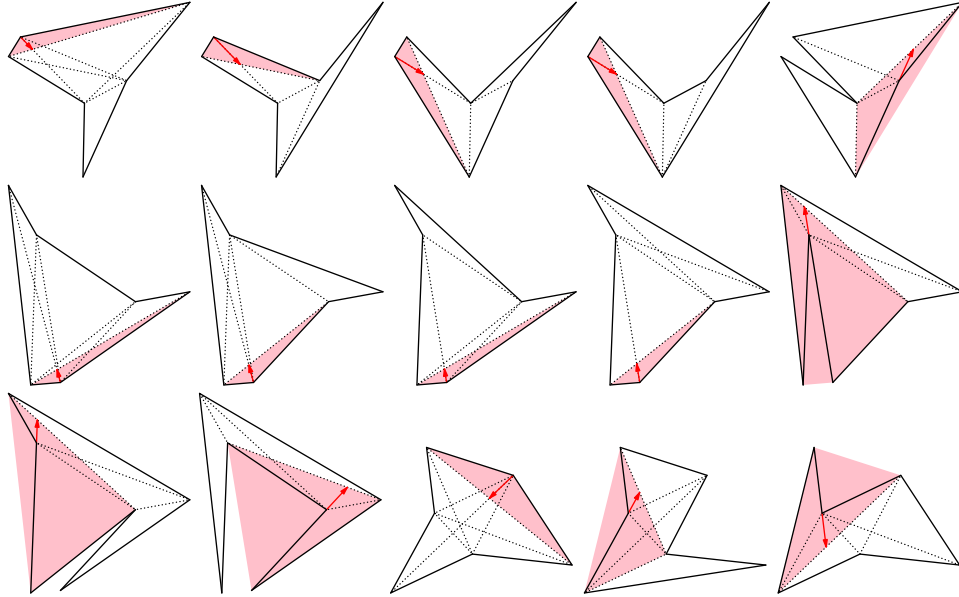
8. N. E. Mnëv, *The universality theorems on the classification problem of configuration varieties and convex polytopes varieties*, Topology and geometry—Rohlin Seminar, Lecture Notes in Math., vol. 1346, Springer, Berlin, 1988, pp. 527–543.
9. J. O’Rourke, *Art gallery theorems and algorithms*, International Series of Monographs on Computer Science, The Clarendon Press, Oxford University Press, New York, 1987.

### A. HEXAGON ENUMERATION

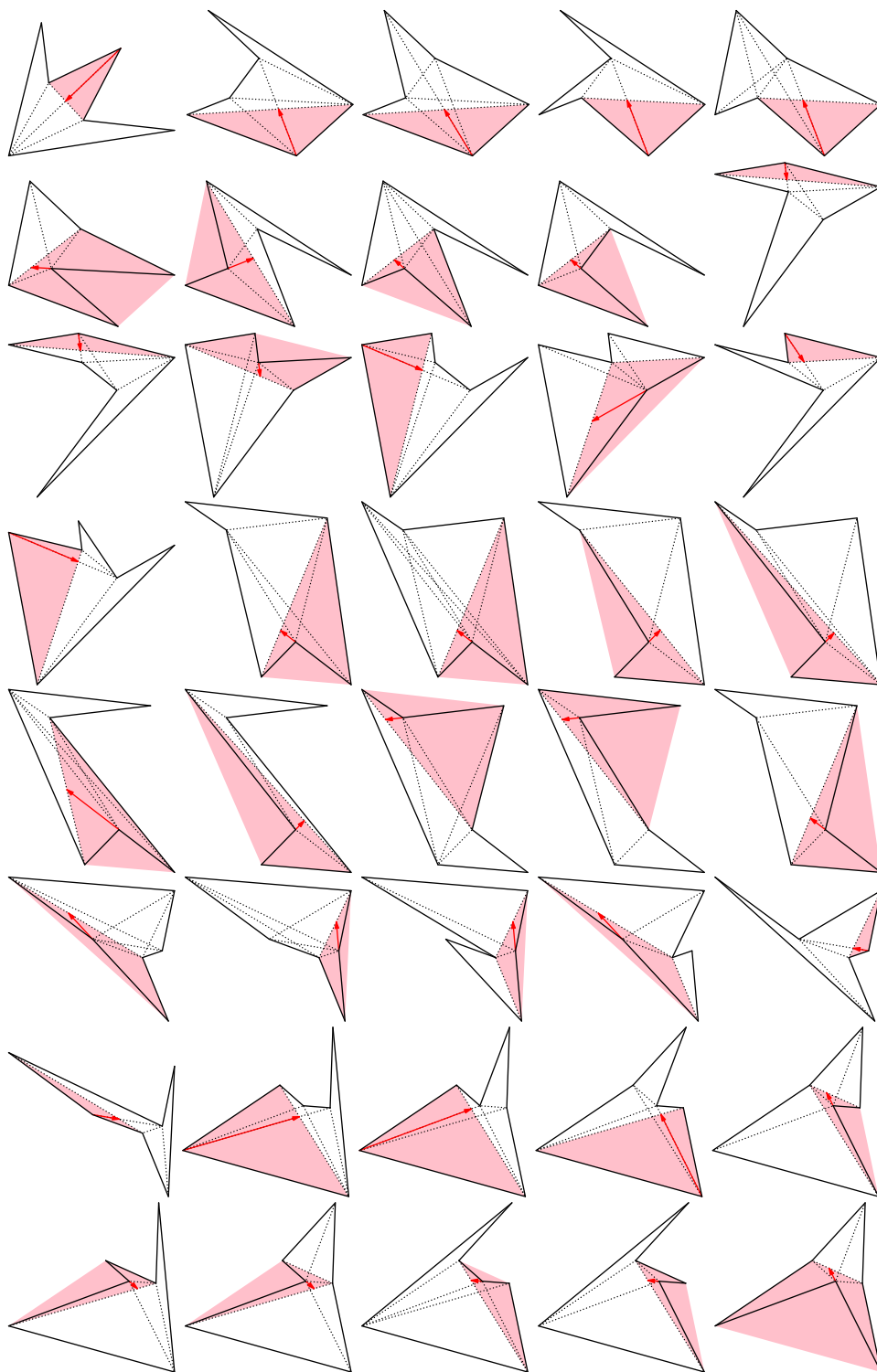
The following figures enumerate the hexagons with two or more reflex vertices from the case analysis of Theorem 6.4. The enumeration includes all such hexagons on general position vertex sets, up to order type. A point set is in general position if no three of its points are incident to a common line. The order type of a point set is a combinatorial structure that encodes, for each ordered triple of distinct points, whether they form a right or left turn (see [7]).

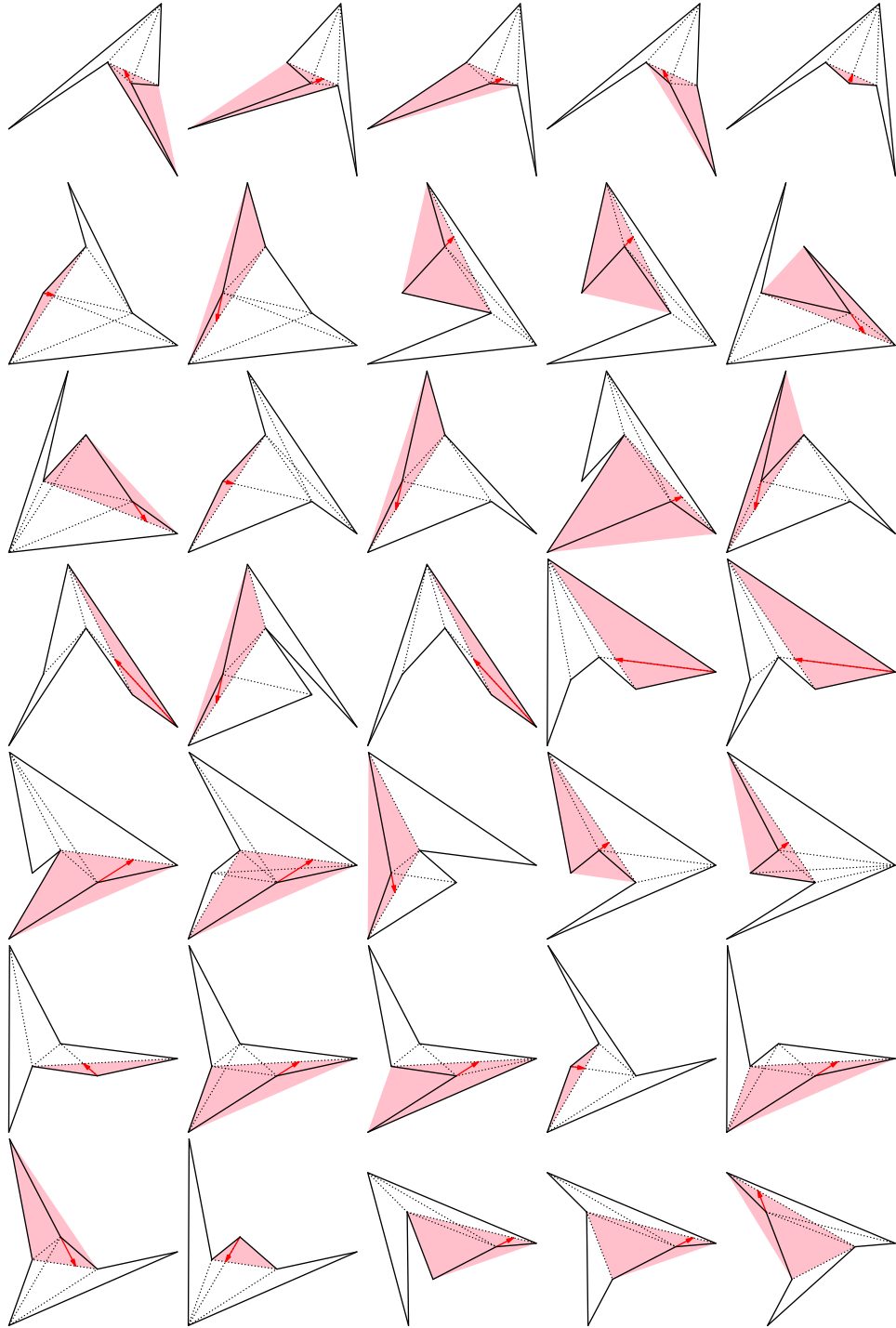
The hexagons were generated by, first, enumerating the Hamiltonian cycles, up to traversal direction, on the complete geometric graphs of each of the sixteen general position point sets of size six from the online order type database of Aichholzer et al.<sup>1</sup> (see [3]). The cycles were then filtered to remove those with edge crossings (non-simple), those without visibility crossings (deflated) and those with less than two reflex vertices.

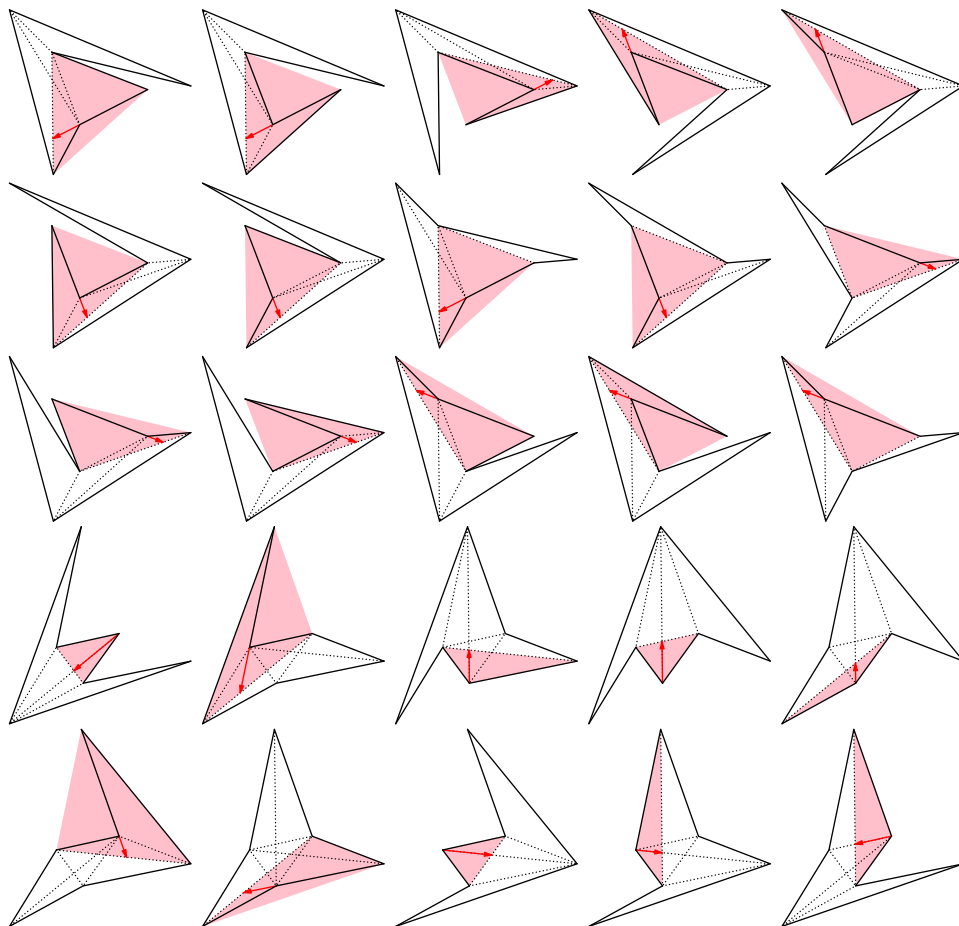
The dotted segments in the figures join visible vertex pairs and the arrows indicate a vertex and a single-segment path along which it may be moved monotonically to reduce the number of visibility crossings of its hexagon by at least one. The shaded region of a figure is the convex polygon  $C$ , as described in the proof of Theorem 6.4.



<sup>1</sup><http://www.ist.tugraz.at/aichholzer/research/rp/triangulations/order-types/>







SCHOOL OF COMPUTER SCIENCE, CARLETON UNIVERSITY  
*E-mail address:* [jit@scs.carleton.ca](mailto:jit@scs.carleton.ca)

SCHOOL OF COMPUTER SCIENCE AND ELECTRICAL ENGINEERING, UNIVERSITY OF  
 OTTAWA  
*E-mail address:* [vida.dujmovic@uottawa.ca](mailto:vida.dujmovic@uottawa.ca)

DEPARTMENT OF MATHEMATICS AND STATISTICS, MCGILL UNIVERSITY  
*E-mail address:* [nima.hoda@mail.mcgill.ca](mailto:nima.hoda@mail.mcgill.ca)

SCHOOL OF COMPUTER SCIENCE, CARLETON UNIVERSITY  
*E-mail address:* [morin@scs.carleton.ca](mailto:morin@scs.carleton.ca)